

# Imprint Control Element-mediated Secondary Methylation Imprints at the *Igf2/H19* Locus\*

Received for publication, August 19, 2002, and in revised form, September 12, 2002  
Published, JBC Papers in Press, September 20, 2002, DOI 10.1074/jbc.M208437200

Madhulika Srivastava‡, Ella Frolova, Brian Rottinghaus, Steven P. Boe, Alexander Grinberg, Eric Lee, Paul E. Love, and Karl Pfeifer

From the Laboratory of Mammalian Genes and Development, NICHD, National Institutes of Health, Bethesda, Maryland 20892

Understanding the molecular basis of monoallelic expression as observed at imprinted loci is helpful in understanding the mechanisms underlying epigenetic regulation. Genomic imprinting begins during gametogenesis with the establishment of epigenetic marks on the chromosomes such that paternal and maternal chromosomes are rendered distinct. During embryonic development, the primary imprint can lead to generation of secondary epigenetic modifications (secondary imprints) of the chromosomes. Eventually, either the primary imprints or the secondary imprints interfere with transcription, leading to parent-of-origin-dependent silencing of one of the two alleles. Here we investigated several aspects pertaining to the generation and functional necessity of secondary methylation imprints at the *Igf2/H19* locus. At the *H19* locus, these secondary imprints are, in fact, the signals mediating paternal chromosome-specific silencing of that gene. We first demonstrated that the *H19* secondary methylation imprints are entirely stable through multiple cell divisions, even in the absence of the primary imprint. Second, we generated mouse mutations to determine which DNA sequences are important in mediating establishment and maintenance of the silent state of the paternal *H19* allele. Finally, we analyzed the dependence of the methylation of *Igf2DMR1* region on the primary methylation imprint about 90 kilobases away.

Mammals inherit two complete sets of chromosomes, one from the mother and one from the father. Most autosomal genes are expressed equivalently from the maternal and the paternal alleles. Imprinted genes, however, are expressed preferentially from only one chromosome in a parent-of-origin-dependent manner (1). Because the active and the inactive promoters of an imprinted gene are present in a single nucleus, the differences in their activity cannot be explained by differences in transcription factor abundance. Rather, the transcription of imprinted genes represents a clear situation in which epigenetic mechanisms restrict gene expression and therefore offers a model for understanding the role of heritable DNA modifications such as cytosine methylation in maintaining appropriate patterns of expression.

The imprinted *Igf2-H19* gene pair is part of a large cluster of

imprinted genes on the distal end of mouse chromosome 7. *H19* and *Igf2* share enhancers and therefore share developmentally complex patterns of gene expression (2). However, they are reciprocally imprinted. *H19* is expressed exclusively from the maternal chromosome, whereas *Igf2* expression is almost entirely paternal in origin (3, 4). The syntenic region in humans on chromosome 11p15.5 is highly conserved in genomic organization and in monoallelic gene expression patterns (5, 6). Loss-of-imprinting mutations at chromosome 11p15.5 are associated with Beckwith-Wiedemann syndrome and with several types of cancer (7–9).

Maternal chromosome-specific expression of *H19* and paternal chromosome-specific expression of *Igf2* are each dependent upon a *cis* acting imprinting control element (*ICE*),<sup>1</sup> a 2-kb region spanning –2 kb to –4 kb upstream of the *H19* promoter (10, 11) (Fig. 1a) and located about 90 kb downstream of *Igf2* (distance based on GenBank™ sequence NW\_000336). However, the mechanisms by which monoallelic expression is maintained at the two loci are distinct (12). *Igf2* is regulated by a methylation-sensitive insulator element that also maps with the *ICE*. This insulator element must be continually present in its unmethylated state to maintain maternal *Igf2* silencing. Repression of paternal *H19* is at least a two-step process. A paternally inherited *ICE* is required in the developing embryo. The primary paternal imprint at the *ICE* somehow induces further epigenetic changes at the locus that silence the paternal *H19* promoter such that the presence of the *ICE* is not subsequently required for maternally restricted transcription in *H19* expressing cells. Thus, at *H19*, the primary imprint established during gametogenesis leads to a secondary imprint responsible for silencing the paternal *H19* (12).

Developmental regulation of cytosine methylation at the *H19* locus is consistent with, and most likely explains, the mechanisms of this two part silencing process. The *ICE* is so far indistinguishable from the *H19DMR* (or *H19* differentially methylated region). Cytosine residues within this 2-kb region are methylated in sperm but not in oocytes (10, 13). This differential methylation survives the global changes in DNA methylation that occur during early mammalian development (14, 15). Post-implantation, the domain of paternal chromosome-specific methylation spreads to include the *H19* promoter and exonic sequences (13, 16, 17). The mechanistic significance of these changes in DNA methylation is evidenced by the correlation between loss of biallelism and gain-of-methylation in the normally developing embryo (18, 19) and also by the loss of *H19* monoallelism in mice carrying a deletion of the DNA methyltransferase gene (20). Mechanisms for this methylation

\* The costs of publication of this article were defrayed in part by the payment of page charges. This article must therefore be hereby marked "advertisement" in accordance with 18 U.S.C. Section 1734 solely to indicate this fact.

‡ To whom correspondence should be addressed: National Institute of Immunology, Aruna Asaf Ali Rd., New Delhi 110067, India. Tel.: 91-11-6162281 or 91-11-6167623 (ext. 482); Fax: 91-11-6162125 or 91-11-6177626; E-mail: madhus@nii.res.in.

<sup>1</sup> The abbreviations used are: ICE, imprinting control element; DMR, differentially methylated region; CFSE, carboxyfluorescein diacetate succinimidyl ester.

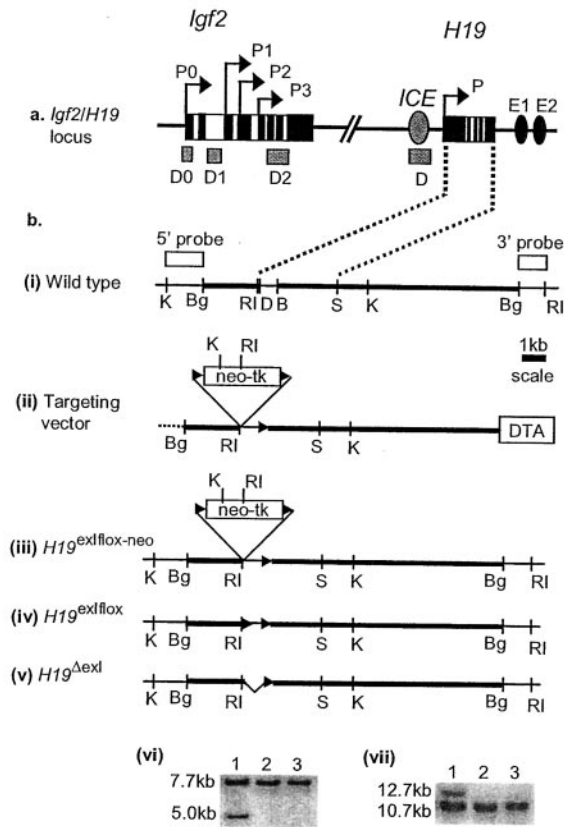


FIG. 1. *a*, schematic diagram of the *Igf2/H19* locus showing the relative positions of the *H19* and *Igf2* genes (rectangles). Transcription start sites are shown as arrows with promoters for *H19* (*P*) and *Igf2* (*P*<sub>0</sub>, *P*<sub>1</sub>, *P*<sub>2</sub>, and *P*<sub>3</sub>) indicated. Exons are shown as blackened areas. Gray rectangles represent differentially methylated regions *H19DMR* (*D*), *Igf2DMR0* (*D*<sub>0</sub>), *Igf2DMR1* (*D*<sub>1</sub>), and *Igf2DMR2* (*D*<sub>2</sub>). The *H19DMR* is coincident with the imprint control element, *ICE* (gray oval), for *H19* and *Igf2*. Shared enhancers (black ovals) for expression of *H19* and *Igf2* in endoderm (*E1*) and skeletal muscle (*E2*) have been defined and are all located downstream of *H19* (2, 32). *b*, strategy for the deletion of a part of *H19* exon I by gene targeting. (i), wild type allele; (ii), targeting vector; (iii), targeted allele, *H19*<sup>ex1lox-neo</sup>; (iv), targeted allele after the excision of the neomycin gene, *H19*<sup>ex1lox</sup>, with *loxP* sites flanking the first 710 bp of *H19*; (v), targeted allele, *H19*<sup>Δex1</sup>, after deletion of *loxP*-flanked region *in vivo* using *E11a-cre* transgenic mice; (vi), correctly targeted clones and *cre* recombinase-mediated excision of neomycin gene were confirmed by Southern hybridization. Genomic DNA from the manipulated embryonic stem cell clones was digested with *KpnI* and hybridized to a 1.5-kb *KpnI*-*BglII* fragment from the region upstream of *H19*. Correctly targeted clones give a 5-kb band from the targeted *H19*<sup>ex1lox-neo</sup> allele and a 7.7-kb band from the wild type allele (lane 1). Subsequent to *cre* recombinase-mediated excision of *neo-tk*, the targeted allele, *H19*<sup>ex1lox</sup>, hybridizes only to the 7.7-kb DNA fragment (lane 2) like the wild type (lane 3); (vii), *EcoRI*-digested genomic DNA hybridized to a 1-kb *BglII*-*EcoRI* fragment downstream of *H19*. Correctly targeted clones show two bands of 12.7 and 10.7 kb from *H19*<sup>ex1lox-neo</sup> and the wild type allele, respectively (lane 1). Subsequent to the excision of *neo-tk*, the *H19*<sup>ex1lox</sup> and the wild type alleles are indistinguishable (lane 2) and resemble the wild type (lane 3). *DTA*, diphtheria toxin gene; *neo-tk*, neomycin resistance and thymidine kinase genes; solid arrowheads, *loxP* sites; thick lines, regions for homologous recombination; white rectangles, regions used as 5' and 3' probes for hybridization; *RI*, *EcoRI*; *B*, *BsmI*; *Bg*, *BglII*; *D*, *DraIII*; *K*, *KpnI*; *S*, *SalI*.

spread are of great interest because of analogies with changes in DNA structure and expression of a number of tumor suppressor genes, as seen in many types of tumor cells.

In this investigation, we examined the silencing of the paternal *H19* promoter and several aspects pertaining to the spread of cytosine methylation. We show first that the cytosine methylation of the *H19* promoter and exonic sequences is stable in the absence of the originating differentially methylated

*ICE* even through mitosis. Second, we have characterized the sequences required to establish and hold this secondary imprint. Finally, we show that the spread of the methylation can occur over long distances, as the paternally methylated *ICE* is responsible for secondary methylation changes that occur about 90 kilobases upstream at the *Igf2* promoter.

#### EXPERIMENTAL PROCEDURES

**Generation of *hCD2-cre* Transgenic Mice**—The plasmid *phCD2-cre*, placing *cre* recombinase under the control of *hCD2* promoter (21), was microinjected into mouse oocytes to obtain the transgenic mice.

**Generation of *H19*<sup>Δex1</sup> Mice**—We used *cre-loxP*-based deletion strategy for generating the mutants (22). As shown in Fig. 1*b*, the targeting vector carried an 11.7-kb *BglII* fragment with *H19* sequences from between -2 and +9.7 kb (all base pairs are described relative to the *H19* transcriptional start site). A *loxP*-flanked cassette with neomycin resistance and thymidine kinase genes (*neo-tk*) was inserted at *DraIII* (+3 bp), and an additional *loxP* site was inserted at *BsmI* (+710 bp). The diphtheria toxin-A gene was inserted for negative selection. Linearized vector was electroporated into mouse RI embryonic stem cells. Correct clones were identified by Southern hybridization. A correctly targeted clone was then re-electroporated with pBS185 (Invitrogen) to direct excision of *neo-tk*, and the excision was detected by Southern hybridization (Fig. 1*b*). Correct clones were injected into C57/BL6-J blastocysts to generate chimeric founder mice that were mated with *E11a-cre* transgenic females (23) to generate strains deleted for exon I (*H19*<sup>Δex1</sup>). The exon I excision was detected by PCR using primers Madhu25 (5'-GAA TTC TGG GCG GAG CCA C-3') and Madhu20 (5'-TGG GAT GTT GTG GCG GCT GG-3') upstream and downstream of the deletion, respectively. The 180-bp PCR product was confirmed by sequencing.

**Isolation, Purification, and Induced Proliferation of T Cells**—Cells were isolated from lymph nodes of +/*DMR*<sup>lox</sup> and +/*DMR*<sup>lox</sup>, *hCD2-cre* mice, suspended in complete RPMI medium, and enumerated. Mature T cells were enriched by depletion of non-T cells with magnetic beads essentially as described (24). The purity of the resulting T cell populations was ≥90%. T cells were then labeled with the membrane-permeable intracellular covalent coupling fluorescent dye carboxyfluorescein diacetate succinimidyl ester (CFSE) as described previously (24). For *in vivo* experiments, labeled cells were resuspended in phosphate-buffered saline (1 × 10<sup>7</sup>/ml) and adoptively transferred into irradiated (T-depleted) hosts by tail vein injection. For *in vitro* experiments, labeled cells were incubated at 37 °C in 12-well plates that had previously been coated with stimulating antibodies (anti-CD3 and anti-CD28). The proliferation of viable cells was assessed by analyzing fluorescence at various time points on a FACScalibur flow cytometer (BD Pharmingen).

**Bisulfite-based DNA Methylation Analysis**—Genomic DNA was digested with restriction enzymes outside the sequence of interest. More specifically, DNA from T cells of +/*DMR*<sup>lox</sup>, *hCD2-cre* (carrying the deletion of *H19DMR*, *DMR*<sup>D</sup>) and skeletal muscle of +/+ and +/*H19*<sup>Δex1</sup> mutants was digested with *BamHI* for analysis of *H19* promoter methylation. DNA from hearts of +/*DMR*<sup>ΔG</sup> and *DMR*<sup>ΔG/+</sup> mutants was digested with *EcoRI* for analysis of *Igf2DMR1* methylation. The DNA was then treated with sodium bisulfite in agarose beads (25). Subsequently the *H19* promoter region or the *Igf2DMR1* region was amplified using a nested PCR strategy such that the primers recognized the bisulfite-converted DNA (Tables I and II). To ensure that the methylation information is derived for several chromosomes from each sample, PCR products from at least three separate PCR reactions were cloned and sequenced for each DNA sample. The parental origin of the sequences obtained was assigned by taking advantage of the polymorphic bases (+167 in the *H19* relative to the transcription start site and -3776 in the *Igf2* relative to the first nucleotide of exon I on the transcript originating from promoter *P*<sub>1</sub>) between *domesticus* and *castaneus* parental alleles.

**Nuclear Run-on Analysis**—Nuclei were isolated from the livers of p8 neonates and prepared as described (26). Briefly, the liver was homogenized in chilled buffer containing 2.1 M sucrose, 10 mM HEPES, pH 7.6, 2 mM EDTA, 15 mM KCl, 10% glycerol, 150 mM spermine, 500 mM dithiothreitol, 500 mM phenylmethylsulfonyl fluoride, and 7 μg/ml aprotinin. Nuclei were pelleted by ultracentrifugation through the same buffer, rinsed, resuspended in buffer containing 40% glycerol, 50 mM Tris-Cl, pH 8.3, 5 mM MgCl<sub>2</sub>, 0.1 mM and EDTA and kept frozen at -70 °C. Typically, nuclei isolated from one liver were resuspended in 450 μl of buffer. The run-on reaction was carried out with 150 μl of nuclei mixed with a buffer containing 10 mM Tris-Cl, pH 8.0, 5 mM MgCl<sub>2</sub>, 300 mM KCl, 1 mg/ml heparin, 1 mM ATP, 1 mM GTP, 1 mM CTP,

and 300  $\mu$ Ci of UTP (800 Ci/mmol) at 30 °C for 30 min with shaking. After DNase and proteinase K treatment, radiolabeled RNA was isolated using Trizol (Invitrogen). Separately, 5  $\mu$ g of linearized plasmid DNA containing the target probes was immobilized on nitrocellulose. RNA equivalent to  $2.5 \times 10^7$  cpm was hybridized to the DNA blot for 40–48 h at 43 °C. The probes for the run-on assay were parts of the *H19* (1.9-kb *PstI-SaI* fragment of *H19*), *Igf2* (first 640 nucleotides of the transcript initiated at P1), and *actin* (region encompassing nucleotides 91–709 of the *actin* cDNA) cloned in pBluescript.

## RESULTS

**Stability of the ICE-mediated Epigenetic Modifications**—Earlier analyses have shown that during embryogenesis, the primary imprint at *H19DMR* directs secondary epigenetic modifications that silence the paternal *H19* promoter (12). We wanted to test whether the acquired epigenetic changes are developmental in nature and stable through mitosis or are lost with cell division and need to be re-established during each cycle of mitosis. Therefore, we deleted the *H19DMR* element in proliferating cells and assayed for the stability of the secondary methylation imprint of the *H19* promoter.

The stability of the secondary imprint was analyzed in T cells, because they retain their proliferative ability even after terminal differentiation. Although T cells do not normally express *H19*, when they are fused with embryonal carcinoma cells, the maternal *H19* locus of the T cells is activated, whereas the paternal *H19* remains silent (27). Also, the *H19DMR* and the *H19* promoter regions are hypermethylated on the paternal chromosome as shown by Southern blot analysis (27). Thus using these two criteria, we concluded that the *H19* locus in the T cells is imprinted.

We generated a transgenic mouse in which the expression of *cre* recombinase was under the control of the human *CD2* (*hCD2*) promoter so that *cre* recombinase was expressed in T cells at an early stage of development (*i.e.* cells that are double negative for cell surface markers CD4 and CD8). Females hemizygous for the *hCD2-cre* transgene were mated with males homozygous for the *DMR<sup>flox</sup>* allele. At the *DMR<sup>flox</sup>* allele, *loxP* sites flank the *H19DMR* and hence *H19DMR* can be deleted dependent upon *cre* expression (12). Thus, the paternal *H19DMR* was expected to be deleted in the T cells of the *+DMR<sup>flox</sup>,hCD2-cre* progeny.

Mature T cells were isolated from the lymph nodes of *+DMR<sup>flox</sup>*

*R<sup>flox</sup>,hCD2-cre* mice and their *+DMR<sup>flox</sup>* nontransgenic littermates. To assay the mitotic stability of the secondary imprint at the *H19* promoter, we induced the isolated T cells to proliferate *in vitro*. We assayed proliferation after 6 days in culture both by counting viable cells and by monitoring changes in CFSE-mediated fluorescence during the *in vitro* culture. CFSE is a nonspecific cell stain. Once a cell is labeled with CFSE, the intensity of fluorescence will depend upon dilution of the dye due to cell division (28). This is clearly evident in adoptive transfer experiments (Fig. 2*a*). CFSE-labeled cells, when transferred to T-depleted hosts, proliferate and have a reduction in fluorescence with each successive division, whereas similar cells transferred to T replete hosts, which do not allow proliferation, exhibit unaltered CFSE fluorescence even after 30 days. By monitoring CFSE fluorescence during *in vitro* culture (Fig. 2*b*) and by counting cells, we projected that the vast majority of T cells had divided at least six times.

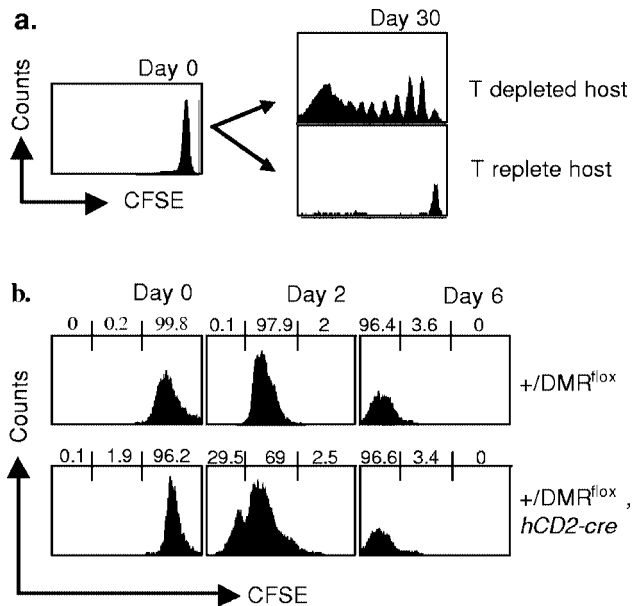


**FIG. 2. CFSE labeling as a measure of cell proliferation.** *a*, purified lymph node T cells from C57BL/6 mice were labeled with the fluorescent dye CFSE (left panel) and injected intravenously into sublethally irradiated (*T depleted*) or nonirradiated (*T replete*) hosts. 30 days after transfer, experimental animals were sacrificed, and lymph node cells were harvested and analyzed by flow cytometry. The right panels show CFSE fluorescence on gated T cell populations. *b*, analysis of proliferation of *in vitro* stimulated T cells by CFSE fluorescence. Purified T cells from *+DMR<sup>flox</sup>* mice (upper panels) or *+DMR<sup>flox</sup>,hCD2-cre* mice (lower panels) were labeled with CFSE and cultured on plates coated with stimulating antibodies. Cells were analyzed for CFSE fluorescence on day 0 (left panels), day 2 (middle panels), and day 6 (right panels) by flow cytometry. The numbers above the graphs represent the percentage of cells in the defined CFSE fluorescence range.

TABLE I  
Primers for the amplification of bisulfite converted DNA

	Region of interest			
	<i>H19</i> promoter		<i>Igf2DMR</i>	
Target allele	DMR <sup>Δ</sup>	wt	<i>H19<sup>Δex1</sup></i>	wt and DMR <sup>ΔG</sup>
First PCR	Madhu90C	Madhu80C	Madhu80C	kep1a
	Madhu84C	Madhu84C	Madhu97C	kep1b
Nested PCR	Madhu81C	Madhu81C	Madhu81C	Madhu110C
	Madhu83C	Madhu83C	Madhu96C	Madhu111C

TABLE II  
Sequences of the primers used for methylation analysis

Primer	Sequence
Madhu80C	5' GTT TTA TGA AGG GTT TTA GTA GGT TA 3'
Madhu81C	5' TTA AGG GAG ATA TTT GGG GAT AAT GTT A 3'
Madhu83C	5' AAC TAT ACC TTC ACT ACC CAA ATC TAA A 3'
Madhu84C	5' CTA CTA CCA ACT ATA CCT TCA CTA CC 3'
Madhu90C	5' TGG AAT TGA TGG TGG TGT TTG TAT TT 3'
Madhu96C	5' CAA ACT AAA CCC ACT ACA ACC TCC TT 3'
Madhu97C	5' TAC CAA ATC CAC TAT AAA CCC TTT CC 3'
kep1a <sup>a</sup>	5' GGA TCT AGA AGT TAA AGT TAG TGG ATA GGT GT 3'
kep1b <sup>a</sup>	5' CCG GAA TTC CAA CTC TTC CCT ACC CCT TAA ACC 3'
Madhu110C	5' TAA AAA CTC TAT AAA CAA CCA CAT AAA A 3'
Madhu111C	5' TGG ATA GGT GTG GGG ATT TAG ATA 3'

<sup>a</sup> kep1a and kep1b include restriction site overhangs for cloning.

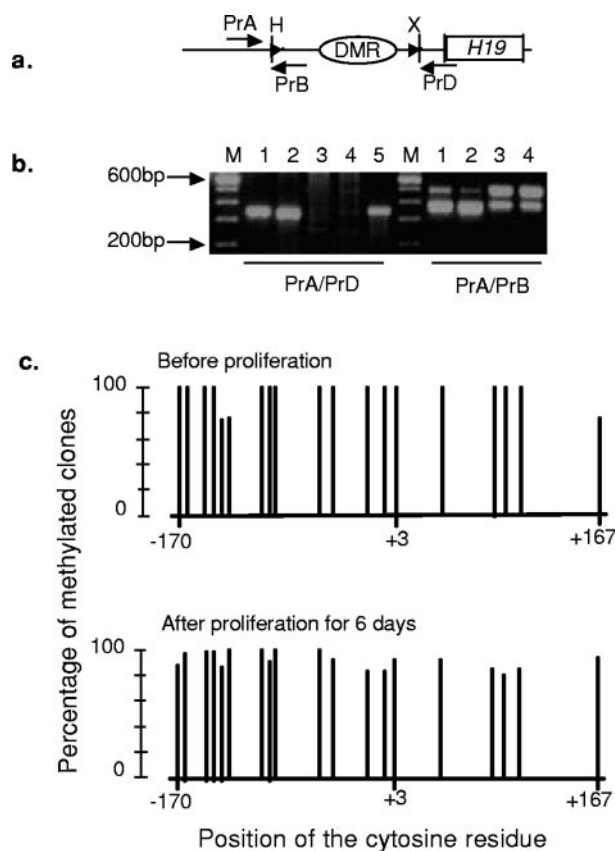


**FIG. 3. Characterization of the stability of the secondary imprint during mitosis in the absence of *H19DMR* in T cells.** *a*, map of the *DMR<sup>lox</sup>* allele showing the relative positions of *H19*, *H19DMR* (*oval*), and the primers used for a PCR-based strategy to detect deletion of the *H19DMR*. Primers A and B (*PrA/PrB*) amplify the region around the  $-7.0$ -kb *HindIII* site to give the 387-bp product from the wild type allele and a 520-bp fragment from the *DMR<sup>lox</sup>* allele. Primers A and D (*PrA/PrD*) generate a 340-bp fragment from the *DMR<sup>D</sup>* allele subsequent to deletion of the *loxP*-flanked region spanning the  $-7.0$ -kb *HindIII* site (*H*) to the  $-0.7$ -kb *XbaI* site (*X*) (12). *Solid triangles*, *loxP* sites. *b*, PCR-based amplification to detect deletion of the *DMR* in T cells of *+/DMR<sup>lox</sup>, hCD2-cre* mice (lanes 1 and 2) and *+/DMR<sup>lox</sup>* mice (lanes 3 and 4). DNA from mouse carrying an *H19DMR* deletion in the germ line (12) was included as a positive control for deletion (lane 5). *M*, DNA size marker; *c*, methylation analysis of the *+/DMR<sup>lox</sup>, hCD2-cre* T cells in the promoter region of *H19* before and after proliferation *in vitro*. Status of methylation at each CpG dinucleotide was analyzed in the  $-170$  to  $+167$ -bp region of the *H19* gene. *Bars* represent the percentage of clones that were found methylated at the specific cytosine residue. The cytosine positions from *left to right* are  $-170$ ,  $-164$ ,  $-147$ ,  $-143$ ,  $-139$ ,  $-131$ ,  $-106$ ,  $-97$ ,  $-94$ ,  $-58$ ,  $-45$ ,  $-20$ ,  $-6$ ,  $+3$ ,  $+44$ ,  $+82$ ,  $+91$ ,  $+102$ , and  $+167$  relative to the transcription start site of *H19* ( $+1$ ). 6 and 15 clones were analyzed from the DNA of cells before and after proliferation, respectively.

As expected, in *+/DMR<sup>lox</sup>, hCD2-cre* transgenic mice, *loxP*-flanked *H19DMR* (Fig. 3*a*) on the paternal chromosome was excised efficiently in the T cells as evidenced by the appearance of a 340-bp deletion-specific product concomitant with a decrease in the *DMR<sup>lox</sup>*-specific 580-bp product (Fig. 3*b*) in the DNA isolated from T cells.

Methylation of the *H19* promoter region was analyzed in the T cells of *+/DMR<sup>lox</sup>, hCD2-cre* mice before and after *in vitro* proliferation (Fig. 3*c*). We used bisulfite sequencing to determine the methylation status of individual cytosine residues of the DNA in the region. Primers were designed to ensure that the information was acquired only from the chromosomes where the *ICE* had been deleted. Like the wild type paternal *H19* promoter (10), the paternal *H19* promoter carrying the *ICE* deletion was hypermethylated. These cells had undergone at least some proliferation *in vivo* as they differentiated into

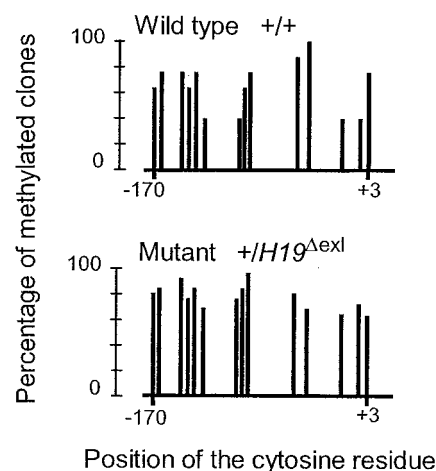


**FIG. 4. Methylation analysis of paternal *H19* promoter region in *+/H19<sup>Δex1</sup>* mutants.** The methylation status at each CpG dinucleotide between  $-170$  and  $+3$  was analyzed by bisulfite sequencing of DNA isolated from skeletal muscle. The *vertical bars* represent the percentage of clones found methylated at the given cytosine position. The cytosine positions from *left to right* are  $-170$ ,  $-164$ ,  $-147$ ,  $-143$ ,  $-139$ ,  $-131$ ,  $-106$ ,  $-97$ ,  $-94$ ,  $-58$ ,  $-45$ ,  $-20$ ,  $-6$ , and  $+3$  relative to the transcription start site of *H19* ( $+1$ ). 8 and 22 clones were analyzed for *+/+* and *+/H19<sup>Δex1</sup>*, respectively.

mature single positive T cells (CD4<sup>+</sup> or CD8<sup>+</sup>). Thus, *H19* secondary imprint survived mitosis *in vivo* despite the absence of *ICE*. The cells that were induced to proliferate extensively *in vitro* also exhibited hypermethylation of the *H19* promoter region comparable with cells before proliferation. This demonstrated conclusively that the absence of *ICE* did not lead to a loss of methylation during mitosis.

Because, subsequent to the *ICE* deletion, there is no loss in methylation despite extensive proliferation *in vivo* or *in vitro*, we concluded that the secondary imprint at the *H19* promoter is stable through mitosis and does not require continuous input from the primary imprint at the *ICE*.

**Requirement of the *H19* Structural Gene for the *ICE* Mediated Epigenetic Silencing**—We next wished to determine which regions of the *H19* gene are essential for acquiring and/or maintaining the secondary imprint that actually represses paternal *H19* transcription. On the wild type paternal chromosome, both the *H19* promoter region and the *H19* RNA coding sequences are hypermethylated (10). In fact, the first exon of *H19* is the most consistently hypermethylated region outside the *H19DMR*. Previous transgenic and knock-in experiments have provided contradictory data regarding the relative importance of these two regions. Deletion of exon I from transgenic constructs results in the loss of transgene imprinting (29). Likewise, replacement of the whole coding region with firefly luciferase also results in biallelic expression of the unmethylated transgene (29). However, replacement of the whole *H19* coding region at the endogenous locus with luciferase results in only sporadic activation upon paternal inheritance (30). Interpreting the luciferase constructions is complicated, and it is not clear whether the presence of luciferase or the absence of the test sequence is the cause for the loss of imprinting. We decided, therefore, to test directly the requirement of *H19* exon I for silencing paternal *H19* promoter. The endogenous *H19* locus was manipulated by gene targeting methods to flank most of exon I with *loxP* sites (Fig. 1*b*). This region was deleted in the germ line using an *EIIa-cre* transgenic line and passed through the maternal and paternal germ lines to analyze the effect of the deletion on methylation of the promoter and on *H19* gene expression.

We analyzed the status of methylation of *H19* promoter by bisulfite sequencing (Fig. 4). The paternal promoters of *H19<sup>Δex1</sup>*

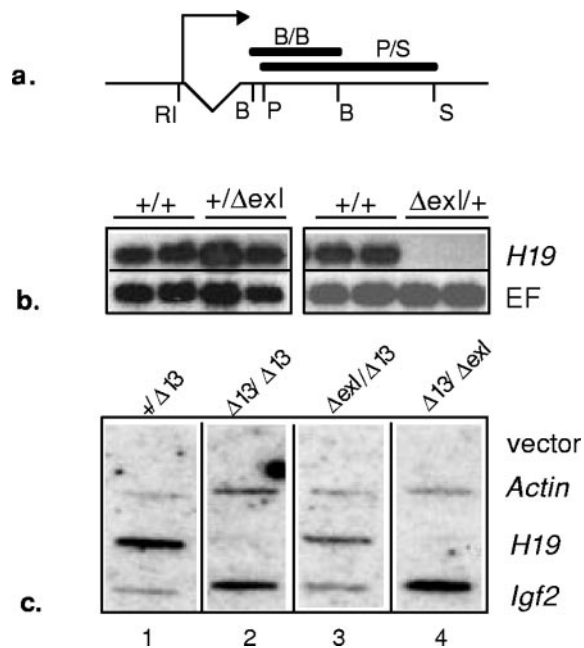


FIG. 5. Expression analysis of *H19* from *H19<sup>ΔexI</sup>* mutants. *a*, regions of *H19* used as probes for Northern analysis (B/B, 1-kb *Bam*HI fragment) and for the nuclear run-on analysis (P/S, 1.9-kb *Pst*I-*Sal*I fragment). *b*, Northern analysis of *H19* RNA from the liver of *+/+*, *+/H19<sup>ΔexI</sup>*, and *H19<sup>ΔexI</sup>/+* neonates. Elongation factor (EF) was detected on stripped blots. *c*, nuclear run-on analysis showing transcriptional initiation of *H19*, *Igf2*, and actin genes in the nuclei of *+/H19<sup>Δ13</sup>* (lane 1), *H19<sup>Δ13</sup>/H19<sup>Δ13</sup>* (lane 2), *H19<sup>ΔexI</sup>/H19<sup>Δ13</sup>* (lane 3), and *H19<sup>Δ13</sup>/H19<sup>ΔexI</sup>* (lane 4).

mutants were consistently hypermethylated like the wild type paternal chromosomes at all of the CpG dinucleotides. Our results clearly demonstrate that although highly methylated itself, exon I of *H19* does not carry any information for the acquisition of methylation on the paternal *H19* promoter.

We wanted to determine whether exon I and its methylation are required to maintain repression of paternal *H19* transcription. We initially attempted to quantitate expression via Northern analysis (Fig. 5*b*). The expression of *H19* in *+/H19<sup>ΔexI</sup>* mutants was similar to the *+/+* control littermates, initially suggesting that paternal *H19* was not appreciably activated because of the deletion. However, maternal deletion mutants (*H19<sup>ΔexI</sup>/+*) also did not exhibit any *H19* expression, suggesting that either the initiation of *H19* transcript or its stability is abolished as a result of the deletion. Keeping this in view, it was clear that Northern analysis was not informative for discerning the effect of the deletion on *H19* imprinting. We performed, therefore, nuclear run-on assays to derive information about the *H19* imprinting in the *H19<sup>ΔexI</sup>* mutants, tentatively assuming that the deletion affects the stability of the transcript rather than its initiation.

To directly test the role of exon I in initiation of transcription, we attempted nuclear run-on experiments, first using nuclei isolated from the livers of *+/H19<sup>Δ13</sup>* and *H19<sup>ΔexI</sup>/H19<sup>Δ13</sup>* mice. (The *H19<sup>Δ13</sup>* mutant removes the entire *H19* promoter and the coding region (31) and thus allowed us to be certain of the parental origin of any transcripts that we measured.) The run-on analyses (Fig. 5*c*, lanes 1 and 3) showed that the mutated *H19<sup>ΔexI</sup>* allele does initiate significant, although reduced, levels of transcription when maternally inherited. Signal strength in a run-on analysis is affected both by alteration in the rate of transcript initiation and by alteration in the stability of the transcript. The reduced *H19* signal in *H19<sup>ΔexI</sup>/H19<sup>Δ13</sup>* mutants could be the result of either one or both of these factors. However, given that transcription initiation was not

entirely abrogated due to exon I deletion and that significant levels of *H19* RNA were observed, it was clear that the run-on analysis could be used to determine the functional necessity of exon I for silencing of paternal *H19*.

We next looked at transcription from the *H19<sup>ΔexI</sup>* allele when it was paternally inherited (Fig. 5*c*, lane 4). Like a wild type paternal allele, the *H19<sup>ΔexI</sup>* chromosome remains silent when paternally inherited. In fact, the levels of transcription could not be distinguished from those noted in nuclei entirely lacking the *H19* gene (Fig. 5*c*, lane 2).

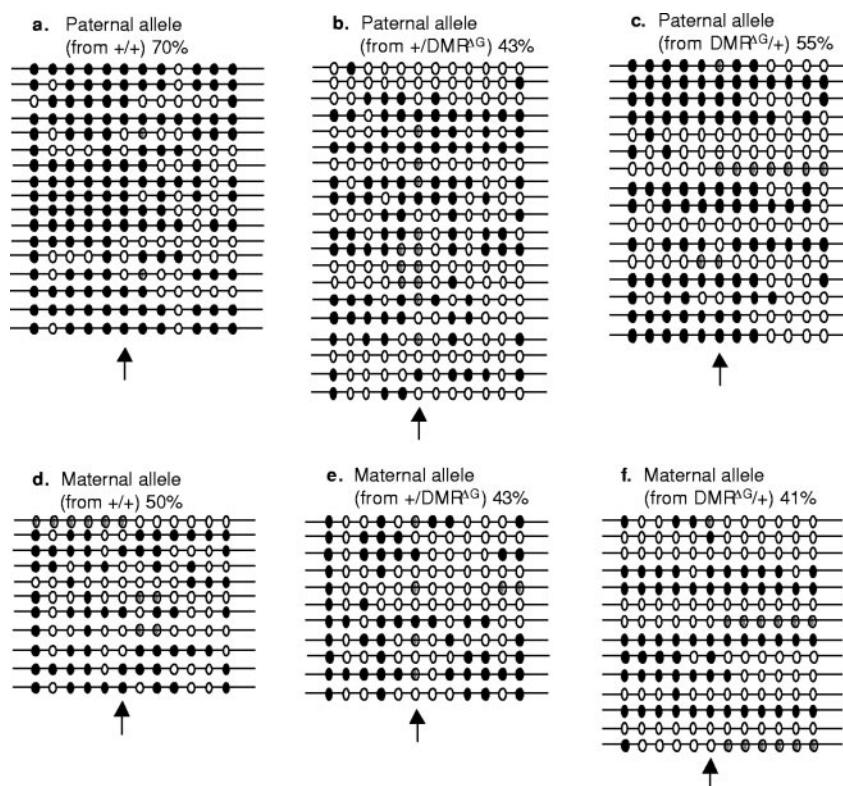
Thus the absence of exon I sequences does not interfere with the *ICE*-mediated silencing of the *H19* promoter. Even though exon I acquires *ICE*-mediated methylation, it is required neither for *ICE*-mediated establishment of the secondary imprint at *H19* promoter nor for its maintenance.

Because *H19<sup>Δ13</sup>* mutation removes the *ICE* in addition to the *H19* gene, use of these mutants allowed us to investigate the effect of the *ICE* on *Igf2* transcription initiation. *ICE* deletion on the maternal chromosome activates normally silent maternal *Igf2* significantly in liver although not to the same levels as the paternal allele (31). However, paternal deletion also reduces *Igf2* expression to some degree (31, 32). In complete accordance with this steady state mRNA data, we observed significant initiation of *Igf2* transcription in *H19<sup>Δ13</sup>/H19<sup>ΔexI</sup>* mutants (Fig. 5*c*, lane 4) where the maternal *Igf2* allele is expected to be active and the paternal *H19<sup>ΔexI</sup>* allele to be fully active. The signals are also intense for *H19<sup>Δ13</sup>/H19<sup>Δ13</sup>* (Fig. 5*c*, lane 2) where both alleles are likely to express but at reduced levels. The initiation is least in *+/H19<sup>Δ13</sup>* and *H19<sup>ΔexI</sup>/H19<sup>Δ13</sup>* mutants (Fig. 5*c*, lanes 1 and 3) where the paternal allele has a reduced expression and the maternal allele is expected to be silent. In other words, the gain of maternal *Igf2* expression seen in maternal *ICE* deletion mutants (like *H19<sup>Δ13</sup>*) is attributed directly to gain of transcriptional initiation on this chromosome.

*Role of the ICE in Methylation of DMR1 at the Igf2 Locus*—Methylation of *Igf2DMR1* located 90 kb upstream of the *H19DMR* has been postulated to play a role in maintaining the expression of *Igf2* (33). Deletion of *Igf2DMR1* indicates that its role is specific to muscle, and it is especially important in maintaining appropriate expression in cardiac muscle (34). We therefore investigated the effect of *H19DMR* on methylation of *Igf2DMR1* in cardiac tissue. We used bisulfite sequencing to derive information about methylation of the *Igf2DMR1* region in DNA isolated from the hearts of wild type *+/+* mice and of mice with a paternally inherited deletion of *H19DMR*, *+/DMR<sup>ΔG</sup>* (12). Examining the 12 CpG residues, we found that the mutant paternal chromosome (Fig. 6*b*) although still methylated was less so than the wild type paternal chromosome (Fig. 6*a*). The extent of methylation, in fact, resembled the wild type maternal chromosome (Fig. 6, *d* and *e*). This clearly indicated that the *ICE* is required for the paternal hypermethylation of *Igf2DMR1* in *cis*. Comparing the methylation status of *Igf2DMR1* in wild type chromosomes from *+/DMR<sup>ΔG</sup>* and *DMR<sup>ΔG</sup>/+* mutants, it appears that the *ICE* deletion also has an effect on *Igf2DMR1* methylation in *trans*, although the effect of paternal *ICE* deletion on *Igf2DMR1* in *cis* is most pronounced.

Given the enormous difference in the expression of *Igf2* from the wild type paternal and the maternal chromosomes, we were surprised to note that the maternal *Igf2DMR1* was also heavily methylated. The methylation was seen at 70 and 50% of the total CpG residues on the paternal and maternal chromosomes, respectively, in the wild type mice (Fig. 6, *a* and *d*). Additionally, no single residue could be identified that was specifically methylated on the paternal chromosome. Both the wild type

**FIG. 6. Methylation analysis of *Igf2DMR1* region as affected by the deletion of *H19DMR* in cis or in trans.** *a* and *d*, wild type (+/+); *b* and *e*, deletion on the paternal chromosome (+/*DMR<sup>ΔG</sup>*); *c* and *f*, deletion on the maternal chromosome (*DMR<sup>ΔG</sup>*/+). The methylation status of 12 CpG dyads of the *Igf2DMR1* region was analyzed by bisulfite sequencing of DNA isolated from heart. Several clones were analyzed for each type of allele under investigation and are presented as a string of circles. Filled circles, methylated CpG; open circles, nonmethylated CpG; hatched circles, noninformative CpG dyad. The numbers with % represent the percentage of CpG residues methylated among those that were analyzed from all of the clones for a specific allele. A vertical arrow represents the CpG dyad that is important for methylation-sensitive GCF2 binding.



paternal and wild type maternal chromosome populations had individual chromosomes that were heavily methylated and others that were practically devoid of any methylation. Deletion of *ICE* on the maternal chromosome activates *Igf2* expression to high levels in the heart (32), and if *Igf2* expression requires *Igf2DMR1* hypermethylation, we would expect hypermethylation of *Igf2DMR1* on the mutant maternal chromosome. Hence, we analyzed the effect of *ICE* deletion on maternal *Igf2DMR1* methylation. However, the extent of methylation on the expressing mutant maternal chromosomes (Fig. 6f) is low, comparable with wild type chromosomes (Fig. 6, *d* and *e*). Thus, comparing maternal and paternal wild type and mutant chromosomes, we see a correlation of methylation of *Igf2DMR1* with a methylated *H19DMR* but not with *Igf2* expression.

#### DISCUSSION

Repression of the paternal *H19* allele is a two-step process. Molecular evidence strongly supports the idea that a paternal imprint at the *ICE* between  $-2$  and  $-4$  kb upstream of the *H19* promoter marks the parental origin of the chromosome (10, 11). Molecular and genetic studies demonstrate that during development this primary *H19DMR* imprint directs further epigenetic changes that actually silence the paternal *H19* promoter (12). These changes certainly involve DNA methylation. Here we demonstrate that the secondary methylation imprint is developmental. That is, it does not require continued signaling from the primary imprint at the *ICE* but is stable even during multiple mitoses.

The *ICE* acts epigenetically to modify the *H19* promoter region and also part of the structural gene. Both of these regions are hypermethylated post-fertilization, and the paternal *H19* promoter is silenced. In fact, the exon I region is most completely and consistently methylated. However, our results here indicate that the region is not required at all for acquiring the secondary imprint. Thus, CpG methylation does not always connote function but in some cases may occur only coincidentally with other changes.

Our results concerning the role of exon I in maintaining *H19*

imprinting are not really consistent with previous transgenic experiments (29). Our personal observation is that transgenic constructs are particularly sensitive to disruptions in imprinting. For example, many transgenes show a copy number dependence in imprinted expression and DNA methylation that is obviously not applicable to the endogenous locus. These experiments perhaps suggest that the imprinting signals may include large DNA structures and elements in a way that is really not yet appreciated. Until recently, most transgenic constructs extended only 4 kb on the 5' flank and therefore included neither the entire *H19DMR* nor all of the CTCF binding sites. Recent experiments from the Bartolomei laboratory (35) indicate that additional flanking DNA may provide copy number and position independence and may provide a better substrate for further mutagenesis of transgene constructs.

Interestingly, the *loxP* sites left downstream to the promoter after our manipulation of the locus were also methylated (data not shown). Thus it appears that any CpG residue at that locus may be modified during the spread of methylation irrespective of its sequence context. This result is consistent with appropriate imprinting of the *NeoR* gene inserted at the *H19* locus (36). Thus, even the sequence of the *H19* promoter may not actually play an important role for methylation spreading but may simply be a CpG-rich element in the right place. We are currently investigating the ability of the *ICE* to modify promoters other than *H19* when they are placed in adjacent position.

Our experiments have also demonstrated that the *ICE* controls the imprinting of *Igf2* at the transcript initiation level despite being 90 kb downstream of the promoter. This is in complete accordance with the presence of a transcriptional insulator at the *ICE* (32, 37, 38). Insulator elements, when present between the enhancer and promoter, prevent the expression of genes. The mechanistic details of the process seem to be diverse and not well understood (39). Our nuclear run-on analysis suggests that the insulator in the *ICE* truly prevents promoter activation and transcript initiation by the enhancer.

Finally, we investigated the role of *H19DMR* in methylation

of the *Igf2DMR1* element. *Igf2DMR1* has been identified as methylated in a parent-of-origin manner (17, 33, 40). Subsequently, its crucial role in maintaining appropriate expression patterns of *Igf2* in mesodermal tissues was demonstrated *in vivo* using embryonic stem cell-generated mutational analyses (34). Further, an *Igf2DMR1*-specific binding protein, GCF2, has been identified in which affinity is dependent upon the levels of CpG methylation (41). Our bisulfite sequencing results are puzzling in this regard because although we see a correlation between *Igf2DMR1* methylation and the presence of a methylated *H19DMR* in *cis*, we do not note a correlation between *Igf2* expression and the methylation of the 12 CpG dyads we examined. Further, investigations are clearly warranted.

Although our experiments do not support a crucial functional role for *Igf2DMR1* methylation, they do confirm and extend previous DNA sequencing experiments indicating that the degree of *Igf2DMR2* methylation was altered *in trans* upon deletion of the *H19DMR* (via the *H19<sup>Δ13</sup>* mutation) (42). These results are intriguing in that they suggest a communication between the maternal and paternal chromosomes sometime after implantation, when the methylation of the *Igf2DMR1* is first established. The idea that imprinted alleles interact and that such interactions are crucial to maintaining monoallelic expression has always been an attractive hypothesis but one with limited experimental support. Paternal and maternal human 15q11-q13 domains interact specifically during S phase (43) although no functional role for the interaction has been subsequently supported. To date no such physical association of the chromosomes has been noted at the *Igf2/H19* locus. We have never found any evidence for transvection (*i.e.* communication between enhancer and promoter elements *in trans* at the *H19* locus) despite specific attempts to record such interactions (44). Finally, *H19* transgenes do not require a partner to exhibit imprinting. Rather single copy hemizygous transgenes exhibit monoallelic expression even in an *H19<sup>Δ13</sup>* genetic background (32). Nonetheless, it is interesting to note that the *ICE* can alter methylation patterns not only 90 kb away but also across other chromosomes.

**Acknowledgments**—We thank Shirley Tilghman for the *H19<sup>Δ13</sup>* mice and Heiner Westphal for the *Ella-cre* mice.

## REFERENCES

- Reik, W., and Walter, J. (2001) *Nat. Rev. Genet.* **2**, 21–32
- Leighton, P. A., Saam, J. R., Ingram, R. S., Stewart, C. L., and Tilghman, S. M. (1995) *Genes Dev.* **9**, 2079–2089
- Bartolomei, M. S., Zemel, S., and Tilghman, S. M. (1991) *Nature* **351**, 153–155
- DeChiara, T. M., Robertson, E. J., and Efstratiadis, A. (1991) *Cell* **64**, 849–859
- Paulsen, M., Davies, K. R., Bowden, L. M., Villar, A. J., Franck, O., Fuermann, M., Dean, W. L., Moore, T. F., Rodrigues, N., Davies, K. E., Hu, R. J., Feinberg, A. P., Maher, E. R., Reik, W., and Walter, J. (1998) *Hum. Mol. Genet.* **7**, 1149–1159
- Paulsen, M., El Maarri, O., Engemann, S., Strodicke, M., Franck, O., Davies, K., Reinhardt, R., Reik, W., and Walter, J. (2000) *Hum. Mol. Genet.* **9**, 1829–1841
- Reik, W., Bowden, L., Constanica, M., Dean, W., Feil, R., Forne, T., Kelsey, G., Maher, E., Moore, T., Sun, F. L., and Walter, J. (1996) *Int. J. Dev. Biol. Suppl.* **1**, 53S–54S
- Sun, F. L., Dean, W. L., Kelsey, G., Allen, N. D., and Reik, W. (1997) *Nature* **389**, 809–815
- Maher, E. R., and Reik, W. (2000) *J. Clin. Invest.* **105**, 247–252
- Tremblay, K. D., Saam, J. R., Ingram, R. S., Tilghman, S. M., and Bartolomei, M. S. (1995) *Nat. Genet.* **9**, 407–413
- Thorvaldsen, J. L., Duran, K. L., and Bartolomei, M. S. (1998) *Genes Dev.* **12**, 3693–3702
- Srivastava, M., Hsieh, S., Grinberg, A., Williams-Simons, L., Huang, S. P., and Pfeifer, K. (2000) *Genes Dev.* **14**, 1186–1195
- Bartolomei, M. S., Webber, A. L., Brunkow, M. E., and Tilghman, S. M. (1993) *Genes Dev.* **7**, 1663–1673
- Warnecke, P. M., Mann, J. R., Frommer, M., and Clark, S. J. (1998) *Genomics* **51**, 182–190
- Rougier, N., Bourc'his, D., Gomes, D. M., Niveleau, A., Plachot, M., Paldi, A., and Viegas-Pequignot, E. (1998) *Genes Dev.* **12**, 2108–2113
- Ferguson-Smith, A. C., Sasaki, H., Cattanaach, B. M., and Surani, M. A. (1993) *Nature* **362**, 751–755
- Brandeis, M., Kafri, T., Ariel, M., Chaillet, J. R., McCarrey, J., Razin, A., and Cedar, H. (1993) *EMBO J.* **12**, 3669–3677
- Ohlsson, R., Hedborg, F., Holmgren, L., Walsh, C., and Ekstrom, T. J. (1994) *Development* **120**, 361–368
- Szabo, P. E., and Mann, J. R. (1995) *Genes Dev.* **9**, 3097–3108
- Li, E., Beard, C., and Jaenisch, R. (1993) *Nature* **366**, 362–365
- Love, P. E., Shores, E. W., Lee, E. J., Grinberg, A., Munitz, T. I., Westphal, H., and Singer, A. (1994) *J. Exp. Med.* **179**, 1485–1494
- Gu, H., Zou, Y. R., and Rajewsky, K. (1993) *Cell* **73**, 1155–1164
- Lakso, M., Pichel, J. G., Gorman, J. R., Sauer, B., Okamoto, Y., Lee, E., Alt, F. W., and Westphal, H. (1996) *Proc. Natl. Acad. Sci. U. S. A.* **93**, 5860–5865
- Feng, C., Woodside, K. J., Vance, B. A., El Khoury, D., Canelles, M., Lee, J., Gress, R., Fowlkes, B. J., Shores, E. W., and Love, P. E. (2002) *Int. Immunol.* **14**, 535–544
- Olek, A., Oswald, J., and Walter, J. (1996) *Nucleic Acids Res.* **24**, 5064–5066
- Milligan, L., Antoine, E., Bisbal, C., Weber, M., Brunel, C., Forne, T., and Cathala, G. (2000) *Oncogene* **19**, 5810–5816
- Forejt, J., Saam, J. R., Gregorova, S., and Tilghman, S. M. (1999) *Exp. Cell Res.* **252**, 416–422
- Parish, C. R. (1999) *Immunol. Cell Biol.* **77**, 499–508
- Pfeifer, K., Leighton, P. A., and Tilghman, S. M. (1996) *Proc. Natl. Acad. Sci. U. S. A.* **93**, 13876–13883
- Jones, B. K., Levorse, J. M., and Tilghman, S. M. (1998) *Genes Dev.* **12**, 2200–2207
- Leighton, P. A., Ingram, R. S., Eggenschwiler, J., Efstratiadis, A., and Tilghman, S. M. (1995) *Nature* **375**, 34–39
- Kaffer, C. R., Srivastava, M., Park, K. Y., Ives, E., Hsieh, S., Batlle, J., Grinberg, A., Huang, S. P., and Pfeifer, K. (2000) *Genes Dev.* **14**, 1908–1919
- Feil, R., Walter, J., Allen, N. D., and Reik, W. (1994) *Development* **120**, 2933–2943
- Constancia, M., Dean, W., Lopes, S., Moore, T., Kelsey, G., and Reik, W. (2000) *Nat. Genet.* **26**, 203–206
- Cranston, M. J., Spinka, T. L., Elson, D. A., and Bartolomei, M. S. (2001) *Genomics* **73**, 98–107
- Ripoche, M. A., Kress, C., Poirier, F., and Dandolo, L. (1997) *Genes Dev.* **11**, 1596–1604
- Bell, A. C., and Felsenfeld, G. (2000) *Nature* **405**, 482–485
- Hark, A. T., Schoenherr, C. J., Katz, D. J., Ingram, R. S., Levorse, J. M., and Tilghman, S. M. (2000) *Nature* **405**, 486–489
- West, A. G., Gaszner, M., and Felsenfeld, G. (2002) *Genes Dev.* **16**, 271–288
- Sasaki, H., Jones, P. A., Chaillet, J. R., Ferguson-Smith, A. C., Barton, S. C., Reik, W., and Surani, M. A. (1992) *Genes Dev.* **6**, 1843–1856
- Eden, S., Constanica, M., Hashimshony, T., Dean, W., Goldstein, B., Johnson, A. C., Keshet, I., Reik, W., and Cedar, H. (2001) *EMBO J.* **20**, 3518–3525
- Forne, T., Oswald, J., Dean, W., Saam, J. R., Bailleul, B., Dandolo, L., Tilghman, S. M., Walter, J., and Reik, W. (1997) *Proc. Natl. Acad. Sci. U. S. A.* **94**, 10243–10248
- LaSalle, J. M., and Lalonde, M. (1996) *Science* **272**, 725–728
- Kaffer, C. R., Grinberg, A., and Pfeifer, K. (2001) *Mol. Cell. Biol.* **21**, 8189–8196